SCIENTIFIC REPORTS

OPEN

SUBJECT AREAS:
BIOPHYSICAL CHEMISTRY
PROTEIN FOLDING
THERMODYNAMICS
KINETICS

Received
14 February 2013

Accepted
8 April 2013

Published
17 June 2013

Correspondence and requests for materials should be addressed to R.M. (maha@iiserb.ac.in)

* These authors contributed equally to this work.

Modulating lipid dynamics and membrane fluidity to drive rapid folding of a transmembrane barrel

Svetlana Rajkumar Maurya*, Deepti Chaturvedi* & Radhakrishnan Mahalakshmi

Department of Biological Sciences, Indian Institute of Science Education and Research, Transit campus: ITI (Gas Rahat) Building, Govindpura, Bhopal 462023. India.

Lipid-protein interactions, critical for the folding, stability and function of membrane proteins, can be both of mechanical and chemical nature. Mechanical properties of lipid systems can be suitably influenced by physical factors so as to facilitate membrane protein folding. We demonstrate here that by modulating lipid dynamics transiently using heat, rapid folding of two 8-stranded transmembrane β-barrel proteins OmpX and OmpA$^{1-171}$, in micelles and vesicles, can be achieved within seconds. Folding kinetics using this 'heat shock' method shows a dramatic ten to several hundred folds increase in refolding rate along with ~100% folding efficiency. We establish that OmpX thus folded is highly thermostable even in detergent micelles, and retains structural characteristics comparable to the protein in bilayers.

Interactions between the lipid environment and membrane proteins are known to play an important role in the function and regulation of the latter, in both native and artificially reconstituted membrane protein systems[1]. It is also becoming increasingly evident that mechanical forces (physical elements of the lipid system such curvature stress, fluidity, packing etc.) associated with the lipid membrane or micelle may also contribute significantly to transmembrane (TM) protein function[2,3], energetics and protein-protein interaction(s) in a lipid-independent manner[4,5]. Folding of TM helices can be thermodynamically facilitated or spontaneous[2,5]; however, TM β-barrels exhibit a slower refolding process *in vitro*, and experimental observations indicate that following rapid adsorption, the rate determining step is barrel insertion into the lipid milieu[6,7]. Achievement of near-complete refolding may take hours to days[7–9], promoting protein aggregation and adversely affecting sample stability.

Based on previous observations[7–11], we speculated that altering physical properties of lipid bilayers and micelles could catalyse the slowest step of the refolding process. With increasing evidence that annular lipids are sufficient to produce stable membrane protein folds[12], harnessing the mechanical dynamics of lipids to accelerate barrel folding can be attempted. We addressed the influence of heat on the folding rate(s) and altered lipid packing efficiency of TM barrels, using *E. coli* Outer membrane protein X (OmpX; H100N mutant[13]) as our model system. OmpX refolding takes several hours to days, is influenced by many factors, and yields varied refolding efficiencies[8,14], with T_{50} or T_m values of ~65°C[14] to ~95°C[15] in vesicles and nanodiscs, respectively. We demonstrate that it is possible to achieve a highly stable and folded form of OmpX within seconds, in micelles and vesicles, by temperature-assisted modulation of lipid dynamics during the protein folding process.

Results

Recombinant OmpX was expressed and purified using reported protocols[8], and initial refolding screens yielded highest efficiency in ~80 mM LDAO micelles, at 4°C. To probe the effect of temperature on folding, refolding reactions were directly subjected to 1 h incubation at various temperatures, and the efficiency was monitored by SDS-PAGE gel mobility shift[8]. The results demonstrated a temperature-dependent increase in folding of OmpX, with peak value at ~70°C (Fig. 1a). Real time monitoring of the folding process using slow heating at both high and low lipid-to-protein ratio (LPRs) achieved using circular dichroism (CD) measurements (Supplementary Fig. 2) was in line with gel experiments.

From interrupted folding measurements, we deduced that complete refolding was achieved within the first few minutes (Fig. 1b and c), with refolding showing a fast (k_{f1}) and slow (k_{f2}) exponential phase of the order of 7.79 ± 1.7 min^{-1} and 0.45 ± 0.2 min^{-1}, arising possibly from rapid barrel insertion and a slow local structural rearrangement, at 70°C. These values are several folds faster than the reported folding kinetics of the order of

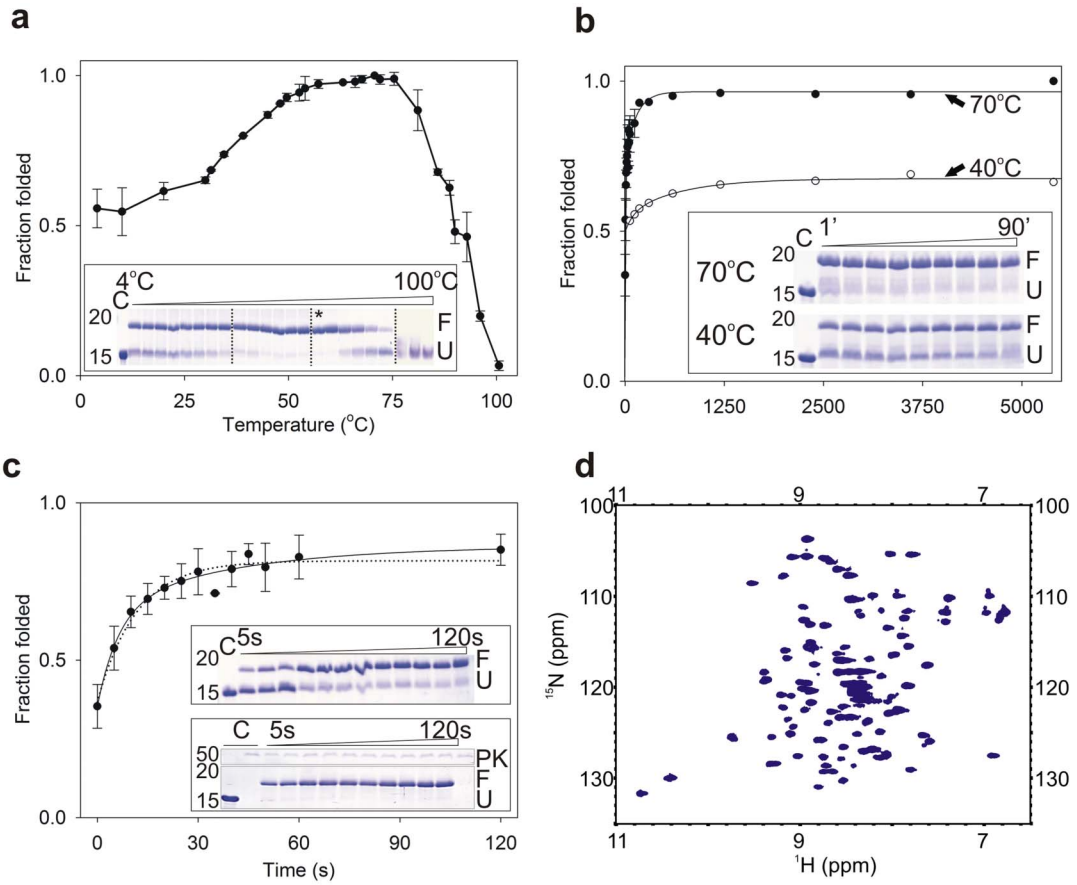

Figure 1 | Temperature modulated OmpX refolding kinetics. (a) Refolding efficiency of OmpX in LDAO monitored with temperature shows highest efficiency at ~70°C (*). OmpX folding kinetics monitored at 40°C and 70°C (b) indicates a fast and slow component at 70°C, which can be fit to a double exponent (solid line). The fast component, monitored separately, is shown with data fitted to double (solid line) and single (dotted line) exponent (c). Inset: Representative gels. C: Unfolded OmpX control; F: Folded OmpX; U: Unfolded OmpX; PK: proteinase K. (d) ^{1}H-^{15}N HSQC of OmpX refolded using heat shock. Inset of Figure 1a shows multiple processed gels separated by dotted lines, and placed together for concise presentation. Original unmodified complete gel images are available in Supplementary Figure 16. All samples were derived from the same experiment and gels were processed in parallel. Molecular weights of protein standards are indicated beside each gel image.

0.01–0.66 min^{-1} for k_{f1} in similar well-studied barrels such as PagP[7], or the suggestive k_{f1}~0.62 min^{-1} for OmpX refolded at 40°C (Fig. 1b), and yields ~100% folded protein. Indeed most barrel proteins show slow refolding in several lipids other than di-lauroylphosphatidylcholine[7,14].

Our data points to a heat-assisted catalysis of the rate-determining step in barrel folding that is lipid and protein concentration independent; the process does not allow for formation of aggregated species (Supplementary Fig. 3–7) and OmpX thus refolded also exhibits resistance to extensive proteolysis (Fig. 1c inset). Unlike previous observations for OmpX[14], our data indicates increase in folding efficiency with temperature; we attribute this observation to the varied refolding time used in previous experiments and speculate that this accelerated refolding process suppresses occurrence of parallel unfolding and/or aggregation events. This is the first report wherein high temperature has been used to drive transmembrane barrel refolding, within a fraction of time. We are tempted to postulate that the process occurs due to alterations in lipid dynamics.

Owing to similarities of this method with the conventional plasmid transformation protocol, we propose the term "heat shock" (HS) for the OmpX refolding process. Following HS, we observed that immediate transfer of the refolding mix to low temperature (4°C) facilitates 'locking' of the protein in the folded form, providing a stable barrel (Supplementary Fig. 4). Solution ^{1}H-^{15}N HSQC of HS-refolded OmpX (HS-OmpX) in LDAO (Fig. 1d) was in good agreement with published data[8], indicating comparable structures for the protein refolded using HS and conventional methods.

Unfolding kinetics monitored between 75–95°C indicated greater thermostability of HS-OmpX (Supplementary Figs. 8 and 9). Thermal denaturation measurement using CD also showed only marginal unfolding of HS-refolded OmpX at temperatures >80°C in both high (Fig. 2a) and low (Fig. 2b) LPRs, unlike reported T_m values using alternative refolding methods[14,15]; complete recovery to the native form could be achieved upon cooling, unlike OmpX in the absence of lipids (Fig. 2c).

DSC measurements of HS-OmpX in LDAO micelles demonstrated a two-state unfolding with a calculated T_m of ~107.5°C (Fig. 2d), which is in line with T_m estimates obtained from extrapolation of the CD thermal melts. Surprisingly, this value is greater than reported T_m even in lipid-like environments[14,15]. Additionally, HSQC measurements acquired over several months in both LDAO and DPC micelles indicated no significant change in the spectra (Supplementary Fig. 10). Such prolonged stability is rare for TM barrels especially in artificially reconstituted micellar systems, and we believe that this is achieved in our case due to (i) local conformational re-arrangement of the barrel to a more stable form, (ii) absence of soluble aggregates that would otherwise nucleate aggregation with time.

Changes in local Trp environment probed using total fluorescence of HS-OmpX also provided a distinct blue shifted $\lambda_{em\text{-}max}$, with

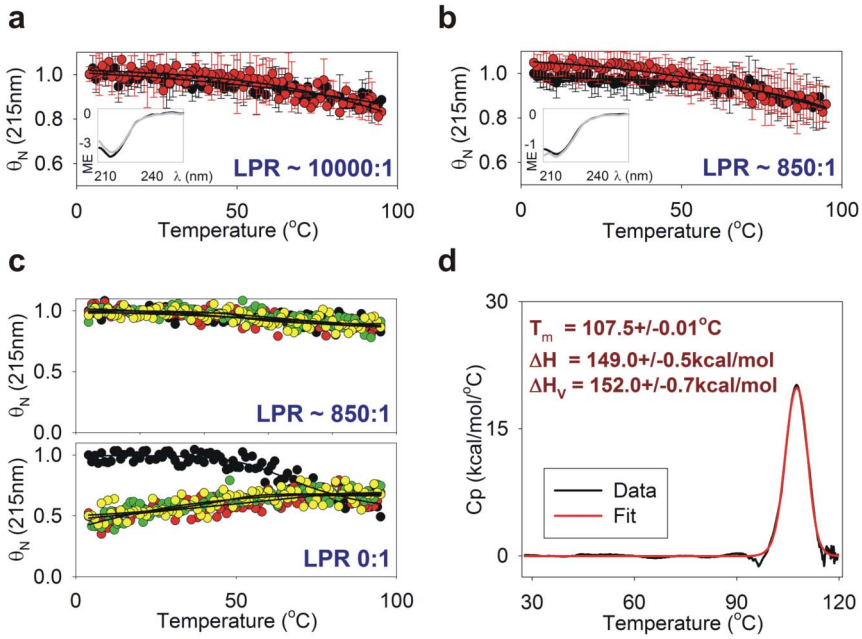

Figure 2 | Thermal denaturation and recovery of HS-OmpX in LDAO monitored using CD at high (a) and low (b) LPR. Inset: CD spectra before (black) and after (grey) denaturation-recovery. (c) Consecutive denaturation-recovery cycles of HS-OmpX in LDAO (top) and OmpX in buffer (bottom). • and • represent denaturation, • and • represent recovery of cycles 1 and 2, respectively. (d) DSC of HS-OmpX.

>60% increase in emission intensity compared to untreated (no HS) sample (Fig. 3a and Supplementary Fig. 11). No further change in emission intensity was observed, indicating that the global and local energy minima were attained after HS (Supplementary Fig. 12). Supporting this conclusion is the blue-shifted poor(er) fluorescence intensity of the slow folding (no HS) sample, indicating that although the adsorption process was completed, OmpX membrane insertion in the absence of temperature-modulated lipid dynamics, was a slow process.

Stability of local packing interactions of HS-OmpX monitored using temperature corrected total fluorescence provided apparent mid points of ~71.0°C and ~57.7°C, for the melting and recovery measurements, respectively, when data were fitted to a two-state equation (Fig. 3b–d and Supplementary Fig. 13). Examination of the crystal structure of OmpX (PDB ID: 1QJ8) indicates the presence of a partially buried W140 that forms local polar contacts with Q11 upon protein folding (Supplementary Fig. 14). We believe that this interaction may quench W140 fluorescence; increasing temperature destabilizes these interactions leading to rise in the total fluorescence. We are tempted to conclude, from this observation, that HS-OmpX adopts a well-folded stable structure that closely resembles the reported crystal structure of OmpX.

Owing to the lack of a distinct red shifted emission even beyond 70°C (Supplementary Fig. 13), we are led to believe that HS-OmpX exists in an equilibrium between folded and a possibly adsorbed state at high temperature, concurrent with CD data that the protein does not undergo complete unfolding. Our fluorescence data also seems to indicate that (i) local unfolding and loss of non-covalent interactions in OmpX are re-established using different mechanisms (ii) the lipid-protein system has different thresholds during heating and cooling processes. It must also be noted that despite complete reversibility, we do not exclude the possible occurrence of hysteresis[5].

We tested the use of 'heat shock' to refold OmpX in various lipids, detergents and lipid/detergent mixtures; gel mobility shifts indicated that refolding efficiency (determined by densitometry) could be improved several fold using HS, in a lipid composition independent manner (Fig. 4). We extended these studies to the transmembrane domain of *E. coli* OmpA (labelled herewith as $OmpA^{1-171}$), which comprises of residues 1–171 of the ~35 kDa protein[6,16]. $OmpA^{1-171}$ exhibits a gel mobility shift profile similar to that of OmpX[16], allowing for assessment of protein folding using SDS-PAGE. We observed that rapid refolding using HS could also be achieved in this protein (Fig. 4), even in conditions such as DMPC, wherein refolding rates are very slow (Supplementary Fig. 15)[6].

Nonetheless, we do not undermine the importance of specific lipid-protein interactions crucial for maintaining the form and function of membrane proteins. For instance, complete refolding was not ubiquitous in all conditions for both proteins using HS (Fig. 4). Hence, preference of β-barrels, and membrane proteins in general, to specific lipid milieu, head groups, chain length, saturation etc., may also serve as key determining factors of overall folding efficiency and long-term stability of the refolded protein in artificially reconstituted systems. The HS method of refolding transmembrane barrels would serve as a rapid screening method to determine which lipid or detergent system is most likely to yield stably folded proteins.

It is also noteworthy that in the heterogeneous lipid/detergent systems (Fig. 4c and d), acceptable amounts of spontaneous OmpX refolding is seen even without heat shock, presumably due to the lipid packing defects introduced by the lipid/detergent mixture. In such cases, HS-driven folding enhances folding efficiency, but not to ~100% in all cases. We are tempted to speculate that while lipid/detergent mixtures with high dynamicity and excessive packing defects facilitate folding, they may also promote the protein unfolding pathway. It is therefore pertinent that, while choosing lipid systems for refolding of membrane proteins, the likelihood of occurrence of the unfolding event also be kept in mind, and those lipid environments be chosen that 'lock' the protein in the folded form.

Discussion

Although rapid barrel refolding is possibly a result of cooperativity between protein and lipid systems, we are tempted to postulate that the protein folding is driven largely due to alteration in lipid dynamics with temperature. We speculate that altering membrane dynamics using temperature may relieve curvature stress by transiently introducing packing defects and thereby reduce the time required for

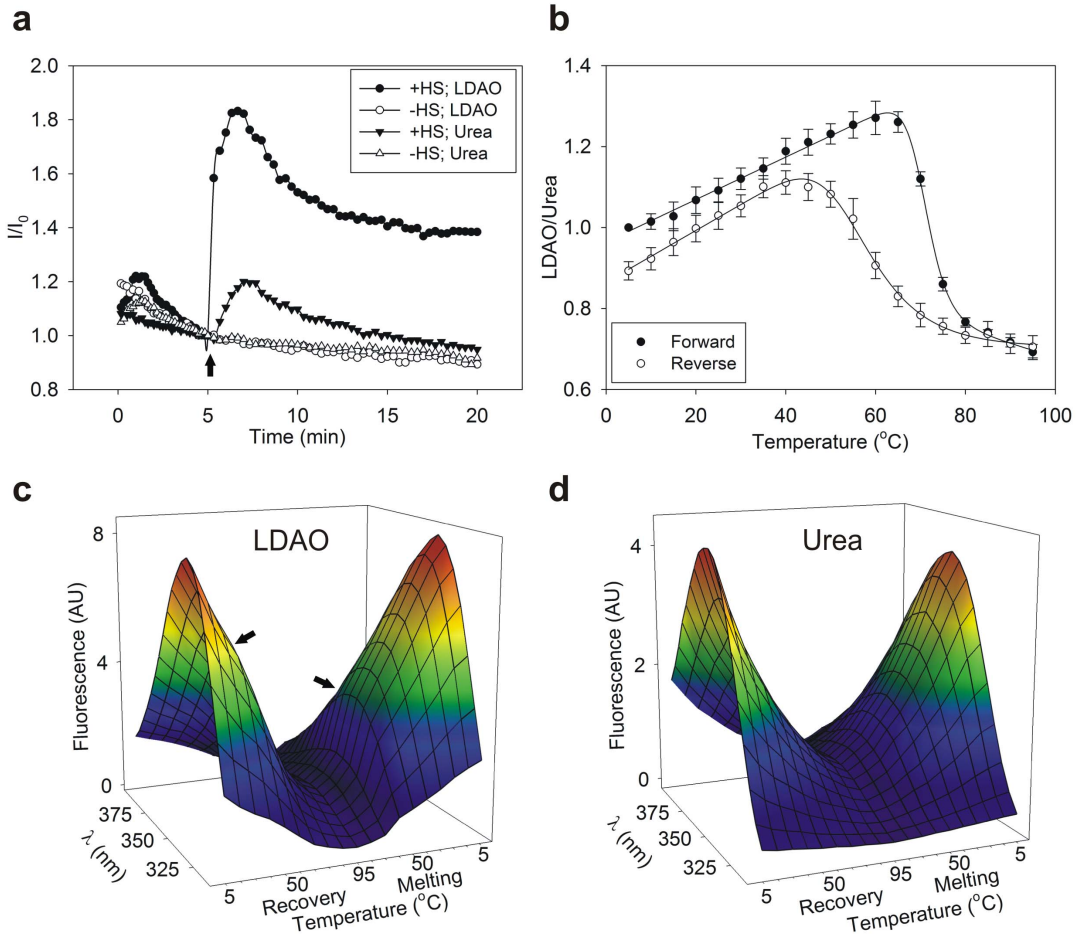

Figure 3 | HS-OmpX stability monitored using total fluorescence. (a) Representative Trp fluorescence of OmpX at 4°C monitored at 338 nm, with and without HS administered at 5 min (I_0, arrow); unfolded OmpX in urea (358 nm) was used as control. (b–d) Changes in local Trp environment of HS-OmpX with temperature. Corrected (b) and absolute (c) fluorescence of HS-OmpX highlighting the non-linear response to temperature (arrows in c). Unfolded OmpX, however, shows a linear dependence (d). Fluorescence intensity in (c) and (d) are factored by 10^5.

membrane insertion and folding of OmpX and $OmpA^{1-171}$; the lack of apparent similarities between outer membrane proteins from mesophiles and thermophiles strengthens our conclusions. Our observation on the generality of heat shock in accelerating refolding, independent of the lipid system suggests that forces governing lipid dynamics are major players in TM barrel folding.

Heat shock can not only enable dramatic reduction in the screening time for membrane protein folding conditions, but also generate a stable and functional barrel; indeed we have observed that a few β-barrels from *Salmonella* sp. can be successfully HS-refolded (data not shown). Our work also supports the increasing evidence that interaction of membrane proteins with their lipid environment is possibly driven largely by mechanical forces, and lipid-specific 'chemical interactions' may be of greater consequence to function, than stability.

Methods

Gene cloning, protein expression and purification, and initial refolding screens are described in the Materials and Methods section of the Supplementary Information (SI). Temperature scan experiments, thermal unfolding, pulse proteolysis, DSC and NMR experiments are also discussed in SI. Unless otherwise specified, final protein concentration used in all reactions is as follows: 1.5 μg/μl (90 μM) OmpX in 20 mM Tris-HCl pH 9.5 containing 80 mM LDAO. This corresponds to a lipid-to-protein ratio (LPR) of ~850 : 1.

Heat shock experiments with interrupted refolding. Optimal temperature required for these experiments was derived from the temperature scans described in SI. Similar sample concentrations and refolding mixture compositions optimized from the initial screens were maintained in these experiments. To derive the minimum time required to achieve complete refolding of the protein at high temperature, interrupted refolding was carried out. The refolding mixture was first pre-incubated for 10 min at 4°C after protein addition; 1 : 20 dilution of urea was maintained, as that of the initial screens. The reaction mix was then quickly transferred to 40°C or 70°C and heated for 1 s–120 min. Samples were then transferred back to 4°C for 15–20 min, following which the reaction was quenched with gel loading dye. Refolding was also directly quenched using the gel loading dye without re-incubation at 4°C. Unboiled samples were examined for refolding efficiency using 15% SDS-PAGE (see Supplementary Fig. 4A for a representative gel). As described in the main text, owing to the brief exposure of the sample to high temperature, this procedure will henceforth be referred to as heat shock (HS).

Optimization of the heat shock (HS) temperature for $OmpA^{1-171}$ was carried out using a similar protocol, with minor modification. Briefly, denatured $OmpA^{1-171}$ was rapidly diluted in pre-chilled refolding reactions containing LDAO, and then subjected to various temperatures ranging from 4°C to 90°C for 3 min only (as described in the temperature scan experiments for OmpX, the initial scans were carried out for 60 min; this was no longer required for $OmpA^{1-171}$). The reaction was stopped using gel loading dye and run on 15% SDS-PAGE. Almost complete refolding was observed at 77°C for $OmpA^{1-171}$ (data not shown); however comparable results were obtained at ~70°C as well (see Figure 4).

Refolding efficiency of both OmpX and $OmpA^{1-171}$ were also screened in various lipids using the HS method. Aliquots of the required amounts of lipids in chloroform were dried in a vacuum concentrator to form thin films; trace amounts of chloroform were removed by overnight lyophilization. Short chain lipids, which form micelles, were re-suspended in MilliQ water, by vortexing. Long chain lipids, which form vesicles, were first hydrated in MilliQ water by continuous vortexing with intermittent incubation at 40°C, to give a milky white suspension. The suspension was sonicated to clarity using a probe sonicator, and small unilamellar vesicles (SUVs) were generated. Titanium dust was removed by centrifugation. Tris-HCl pH 9.5 was later added to obtain a final concentration of 20 mM buffer. Lipids thus prepared were used the same day. The concentrations of the different detergents or lipids used were: 80 mM LDAO, 100 mM β-OG, 60 mM DHPC (1,2-dihexanoyl-*sn*-glycero-3-phosphocholine), 45 mM D7PC (1,2-diheptanoyl-*sn*-glycero-3-phosphocholine),

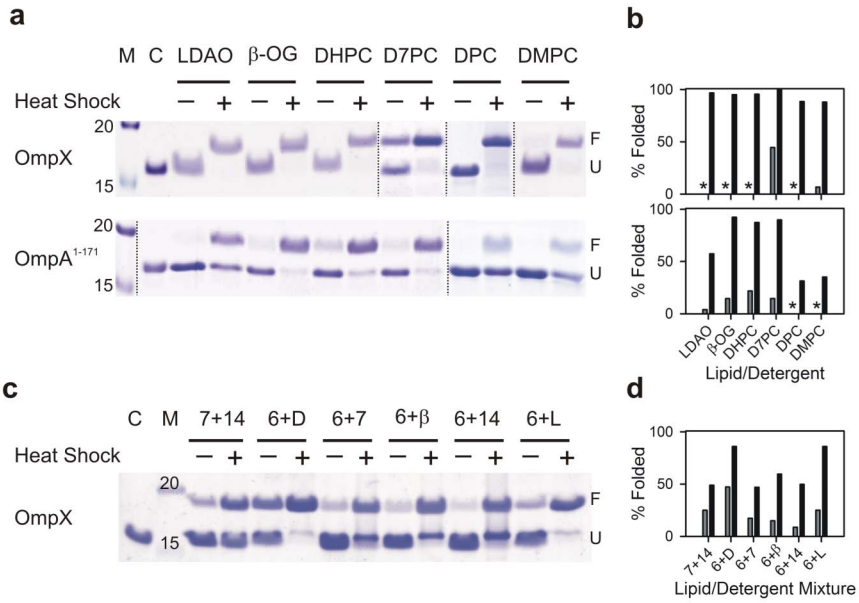

Figure 4 | Refolding of OmpX and OmpA$^{1-171}$ in various lipids, detergents and lipid/detergent mixtures without (−) and with (+) heat shock. Representative SDS-PAGE images (a and c) and corresponding histograms of % folded (b and d) OmpX and OmpA$^{1-171}$ in various lipids or detergents (a and b) and lipid/detergent mixtures (c and d). Fraction folded (calculated as described in methods), obtained without or with heat shock are indicated by grey and black bars, respectively, in (b) and (d). Figure 4a shows multiple processed gels separated by dotted lines, and placed together for display purposes. Original unmodified complete gel images are available in Supplementary Figure 17. All samples were derived from the same HS experiment and gels were processed in parallel, along with their respective controls. M: Marker; C: unfolded protein control; LDAO,L: lauryldimethylamine oxide; β-OG,β: n-octyl-β-D-glucoside; DHPC,6: 1,2-dihexanoyl-sn-glycero-3-phosphocholine; D7PC,7: 1,2-diheptanoyl-sn-glycero-3-phosphocholine; DPC,D: n-dodecylphosphocholine; DMPC,14: 1,2-dimyristoyl-sn-glycero-3-phosphocholine; F: Folded OmpX or OmpA$^{1-171}$; U: Unfolded OmpX or OmpA$^{1-171}$; * Value <1%.

45 mM DPC (*n*-dodecylphosphocholine) and 45 mM DMPC (1,2-dimyristoyl-*sn*-glycero-3-phosphocholine). In the refolding experiments wherein mixtures of lipids/detergents were used, the concentrations of each of the lipids were halved in the final reaction, while maintaining original protein concentrations. As described earlier, all refolding reactions were initiated by the rapid 1 : 20 dilution of OmpX or OmpA$^{1-171}$ in 8 M urea, into the lipid/detergent mixture. Protein stock concentration for both OmpX and OmpA$^{1-171}$ in 8 M urea was adjusted to 30.0 μg/μl, so that the final concentration in the refolding reaction would be 1.5 μg/μl. OmpX and OmpA were quantified using absorbance at 280 nm, using molar extinction coefficients of 34840 M^{-1} cm^{-1} and 46870 M^{-1} cm^{-1}, respectively. The sample was incubated at 4°C for 10 min and heat shock administered at 70°C for 3 min. After re-incubation of these samples at 4°C for 10 min, the reaction was quenched by the addition of SDS-PAGE gel loading dye. In the case of DMPC, 4°C could not be used, since at this temperature, rapid conversion of SUVs to large unilamellar and multilamellar vesicles was observed. Instead, samples were incubated at 10°C and after heat shock, returned to the same temperature.

Gel quantitation and data analysis. Densitometry of all PAGE experiments was performed using UVP Vision Works LS software v6.8 using manufacturer's instructions. Fraction folded was determined using the equation:

$$\text{Fraction folded} = \frac{\text{Folded band intensity}}{\text{Folded band intensity} + \text{Unfolded band intensity}}$$

All the bands were subtracted for background intensity. Fraction folded was normalized to the end point of each reaction, assuming that complete refolding was achieved by then. Data in Figure 1A were normalized to the 70°C data point.

Plots of the folding or unfolding data obtained from SDS-PAGE experiments were generated using SigmaPlot v11.0. Data were fitted to a single exponential function using the formula $y = A_0 + A_1 (1 - e^{-kf1t})$. Double exponents ($y = A_0 + A_1 (1 - e^{-kf1t}) + A_2 (1 - e^{-kf2t})$) were used when optimal fits were not obtained with the single exponent, as described earlier[17]. k_{f1} and k_{f2} represent the folding rates of the fast and slow exponents, respectively.

The data was averaged over at least three independent experiments, and the mean has been represented in most figures. Error bars correspond to standard deviations, calculated using SigmaPlot v11.0. Error bars in some supplementary figures are not shown for purposes of picture clarity. In cases wherein representative data is shown, results were verified using at least three independent experiments.

Fluorescence measurements and heat shock experiments. Fluorescence experiments were carried out on Fluoromax-4C spectrofluorometer (Horiba Jobin Yvon, France). Fluorescence scans were acquired using an excitation wavelength of 295 nm and the emission was recorded from 310 nm to 400 nm (Supplementary Fig. 11). Both the excitation and emission slit widths were kept at 2.5 nm, with an integration time of 0.1 s. Protein concentrations used were adjusted to minimize contribution from inner filter effect; all spectra were buffer subtracted and corrected for dark counts. The final sample had an LPR of ~850 : 1 and contained 14 mM LDAO, 0.25 μg/μl protein and 400 mM urea in 20 mM Tris-HCl pH 9.5. The cuvette chamber was maintained at the desired temperature by an air-cooled peltier. Heat shock was achieved by transferring the cuvette directly to a water bath pre-set at 70°C for 3 min, and immediately placing it in the cuvette chamber for further acquisition.

For the variable temperature experiments, emission was recorded at two wavelengths: 338 nm (emission maximum of the folded species) and 355 nm (emission maximum of the unfolded species). After initiation of refolding in LDAO, an equilibration time of 5 min was given to achieve a stable fluorescence baseline, after which heat shock was administered to the refolding reaction at 70°C using a water bath. The sample was immediately returned to the cuvette chamber and recording was continued at the desired temperature (4, 24, 40, 70 or 95°C) on the fluorometer (Supplementary Fig. 12).

Thermal melting experiment was carried out by recording emission scans between 5°C–95°C, with an increment of 5°C. An equilibration time of 4 min was provided at every temperature, for stabilization. This time also allowed for correlation of the fluorescence data with the CD thermal melt experiments described below. All fluorescence intensities were corrected for temperature dependence of signal intensity, using emission maxima of the unfolded protein in urea (Supplementary Fig. 13). Assumption was made that pH-dependence of Tris HCl did not substantially affect the data and interpretations (effect of pH on refolding was assessed independently as described earlier). Data were fitted to a two state equation[18], using SigmaPlot v11.0.

Circular dichroism (CD) experiments. CD spectra and thermal melting experiments were recorded on a JASCO J-815 spectropolarimeter (JASCO Inc., Japan) equipped with a water-cooled peltier. Two sample conditions with lipid-to-protein ratios (LPR) of ~850 : 1 and ~10000 : 1 were examined. Samples with LPR ~850 : 1 were prepared by directly refolding the protein, using heat shock, in the desired concentrations such that the final refolding mix contained 0.25 μg/μl protein, 14 mM LDAO and 400 mM urea. These concentrations resembled sample conditions used for fluorescence experiments. The latter LPR (~10000 : 1) sample was prepared by diluting the ~850 : 1 mix to final concentrations of 0.08 μg/μl protein, 50 mM LDAO and ~13 mM urea. This process served the dual purpose of increasing the lipid content of the reaction while lowering the urea amounts; protein was therefore anticipated to be more stable in this condition. CD spectra were recorded using a 1 mm path length quartz cell with 0.5 nm bandwidth, 1 s response time and 100 nm/min scan rate.

Thermal denaturation experiments were carried out between 4°C–95°C; temperature was maintained between 0.1°C of the set values using a peltier controller. Sampling was done at an interval of 1°C with 1°C/min ramp rate and the signal was monitored at 208 nm, 215 nm and 222 nm. Experimental parameters for the thermal denaturation experiments were also used to monitor slow refolding kinetics of OmpX (see Supplementary Fig. 2). Samples were prepared by rapid dilution of OmpX in urea into the refolding mixture containing LDAO at 4°C but not subjected to heat shock refolding. Protein, lipid and LPRs used were as described earlier (for samples with heat shock). CD spectra were recorded immediately after initiation of the refolding reaction from 4°C–95°C in steps of 1°C. In all these experiments, it was again assumed that pH variations of Tris HCl did not significantly affect the results.

Each spectrum was blank subtracted for the respective wavelengths. The raw data was converted to molar ellipticity using the formula:

$$[\theta]_{ME} = \frac{\theta}{10 \times c \times 1}$$

where $[\theta]_{ME}$ is the molar ellipticity (deg cm²/dmol), θ is the observed ellipticity (mdeg), c is molar concentration (mol/l), and l is the path length in cm. All CD data were processed using Spectra Manager v2.0 (JASCO Corporation); plots and fits were generated using SigmaPlot v11.0.

To monitor reversibility of unfolding, parameters similar to thermal denaturation experiments were used. Data were first recorded by heating and then cooling the sample from 4°C–95°C–4°C, at ramp rate of 1°C/min, and the process was repeated to obtain data for the re-melting and cooling. No incubation period was given at the start and end temperatures; however, wavelength scans were acquired before and after the first and the second melting, at 4°C. All parameters were kept identical across the experiment(s) and were similar to those described above. Three sets of samples were examined: (i) Refolded OmpX: 0.25 μg/μl OmpX in 20 mM Tris HCl pH 9.5 in 14 mM LDAO, containing 400 mM urea (this condition corresponds to the default sample used in other experiments, including fluorescence measurements) (ii) Unfolded OmpX prepared by rapid dilution of OmpX stock protein in 8 M urea into 20 mM Tris HCl pH 9.5 to obtain 0.25 μg/μl protein in 400 mM urea (iii) Unfolded OmpX obtained by direct re-suspension of the lyophilized protein powder in 20 mM Tris HCl pH 9.5 using vigorous vortexing and sonication, followed by centrifugation to remove the undissolved material; a final OmpX concentration of 0.27 μg/μl was obtained in the buffer. All data were blank subtracted as described earlier. Data analysis and plot generation was carried out using SigmaPlot v11.0. Samples were checked on SDS-PAGE gels before and after each experiment, for possible protein degradation.

1. Lee, A. G. Biological membranes: the importance of molecular detail. *Trends Biochem. Sci.* **36**, 493–500 (2011).
2. Booth, P. J. & Curnow, P. Folding scene investigation: membrane proteins. *Curr. Opin. Struct. Biol.* **19**, 8–13 (2009).
3. Phillips, R., Ursell, T., Wiggins, P. & Sens, P. Emerging roles for lipids in shaping membrane-protein function. *Nature* **459**, 379–385 (2009).
4. Charalambous, K. *et al*. Engineering de novo membrane-mediated protein-protein communication networks. *J. Am. Chem. Soc.* **134**, 5746–5749 (2012).
5. Harris, N. J. & Booth, P. J. Folding and stability of membrane transport proteins in vitro. *Biochim. Biophys. Acta* **1818**, 1055–1066 (2012).
6. Kleinschmidt, J. H. & Tamm, L. K. Secondary and tertiary structure formation of the beta-barrel membrane protein OmpA is synchronized and depends on membrane thickness. *J. Mol. Biol.* **324**, 319–330 (2002).
7. Huysmans, G. H., Baldwin, S. A., Brockwell, D. J. & Radford, S. E. The transition state for folding of an outer membrane protein. *Proc Natl Acad Sci U S A* **107**, 4099–4104 (2010).
8. Mahalakshmi, R., Franzin, C. M., Choi, J. & Marassi, F. M. NMR structural studies of the bacterial outer membrane protein OmpX in oriented lipid bilayer membranes. *Biochim. Biophys. Acta.* **1768**, 3216–3224 (2007).
9. Dewald, A. H., Hodges, J. C. & Columbus, L. Physical determinants of beta-barrel membrane protein folding in lipid vesicles. *Biophys. J.* **100**, 2131–2140 (2011).
10. Pocanschi, C. L. *et al*. The major outer membrane protein of Fusobacterium nucleatum (FomA) folds and inserts into lipid bilayers via parallel folding pathways. *J. Mol. Biol.* **355**, 548–561 (2006).
11. Devaraneni, P. K., Devereaux, J. J. & Valiyaveetil, F. I. In vitro folding of KvAP, a voltage-gated K+ channel. *Biochemistry* **50**, 10442–10450 (2011).
12. Lee, A. G. How lipids and proteins interact in a membrane: a molecular approach. *Mol. Biosyst.* **1**, 203–212 (2005).
13. Mahalakshmi, R. & Marassi, F. M. Orientation of the Escherichia coli outer membrane protein OmpX in phospholipid bilayer membranes determined by solid-State NMR. *Biochemistry* **47**, 6531–6538 (2008).
14. Burgess, N. K., Dao, T. P., Stanley, A. M. & Fleming, K. G. Beta-barrel proteins that reside in the Escherichia coli outer membrane in vivo demonstrate varied folding behavior in vitro. *J. Biol. Chem.* **283**, 26748–26758 (2008).
15. Hagn, F., Etzkorn, M., Raschle, T. & Wagner, G. Optimized Phospholipid Bilayer Nanodiscs Facilitate High-Resolution Structure Determination of Membrane Proteins. *J. Am. Chem. Soc.* (2013).
16. Arora, A., Rinehart, D., Szabo, G. & Tamm, L. K. Refolded outer membrane protein A of Escherichia coli forms ion channels with two conductance states in planar lipid bilayers. *J. Biol. Chem.* **275**, 1594–1600 (2000).
17. Huysmans, G. H., Radford, S. E., Baldwin, S. A. & Brockwell, D. J. Malleability of the folding mechanism of the outer membrane protein PagP: parallel pathways and the effect of membrane elasticity. *J. Mol. Biol.* **416**, 453–464 (2012).
18. Jackson, S. E. & Fersht, A. R. Folding of chymotrypsin inhibitor 2. 1. Evidence for a two-state transition. *Biochemistry* **30**, 10428–10435 (1991).

Acknowledgements

The authors thank M. Patel for help with the LDAO gradient. DSC measurements were carried out by Wipro GE Healthcare (India). Special thanks to Dr. S. Sistla (GE) for help with DSC data analysis and Dr. V. Jain (IISER Bhopal) for help with fluorescence measurements. This work is supported by the Department of Biotechnology, Govt. of India award number BT/HRD/35/02/25/2009. S.R.M. is supported by a research fellowship from CSIR India and D.C. from IISER Bhopal. R.M. is a recipient of the Ramalingaswami fellowship from DBT, Govt. of India.

Author contributions

R.M. conceived the study and designed the overall strategy; S.R.M. and D.C. carried out the experiments. R.M. wrote the manuscript with input from S.R.M. and D.C.

Additional information

Supplementary information accompanies this paper at http://www.nature.com/scientificreports

Competing financial interests: The authors declare no competing financial interests.

How to cite this article: Maurya, S.R., Chaturvedi, D. & Mahalakshmi, R. Modulating lipid dynamics and membrane fluidity to drive rapid folding of a transmembrane barrel. *Sci. Rep.* **3**, 1989; DOI:10.1038/srep01989 (2013).